Sedimentology (1983) **30**, 655–668

The use of the fractal dimension to quantify the morphology of irregular-shaped particles

J. D. ORFORD *and* W. B. WHALLEY

Department of Geography, Queen's University, Belfast BT7 1NN, Northern Ireland

ABSTRACT

For several decades, sedimentologists have had difficulty in obtaining an efficient index of particle form that can be used to specify adequately irregular morphology of sedimentary particles. Mandelbrot has suggested the use of the fractal dimension as a single value estimate of form, in order to characterize morphologically closed loops of an irregular nature. The concept of fractal dimension derives from Richardson's unpublished suggestion that a stable linear relationship appears when the logarithm of the perimeter estimate of an irregular outline is plotted against the logarithm of the unit of measurement (step length). Decreases in step length result in an increase in perimeter by a constant weight (b) for particles whose morphological variations are the same at all measurement scales (self-similarity). The fractal dimension (D) equals 1·0-(b), where b is the slope coefficient of the best-fitting linear regression of the plot. The value of D lies between 1·0 and 2·0, with increasing values of D correlating with increasing irregularity of the outline. In practice, particle outline morphology is not always self-similar, such that two or possibly more fractal elements can occur for many outlines. Two fractal elements reflect the morphological difference between micro-scale edge textural effects (D_1) and macro-scale particle structural effects (D_2) generated by the presence of crenellate-edge morphology (re-entrants). Fractal calibration on a range of regular/irregular particle outline morphologies, plus examination of carbonate beach, pyroclastic and weathered quartz particles indicates that this type of analysis is best suited for morphological characterization of irregular and crenellate particles. In this respect, fractal analysis appears as the complementary analytical technique to harmonic form analysis in order to achieve an adequate specification of all types of particles on a continuum of irregular to regular morphology.

INTRODUCTION

Considerable difficulty has been experienced by sedimentologists in obtaining efficient indices of particle form which also prove effective in the process characterization of sediments (Winkelmolen, 1982). The problem of particle characterization is compounded by the fact that very few detrital particles exhibit a constant regularity on par with regular geometrical solids used as reference forms. As few particles show such regularity, there is a need for a form index which is capable of characterizing the morphology of irregular particles. This paper examines the structure and use of the fractal dimension (Mandelbrot, 1977) as a means by which such irregular particle morphological profiles can be quantified.

In this paper, the general term form is used to denote 'the expression of the external morphology of the object' (Whalley, 1972). Components of form include the traditional sedimentological measures of shape, sphericity ('circularity' in two dimensions), angularity, roundness as well as surface texture.

THE PROBLEM OF MEASURING IRREGULAR PARTICLE MORPHOLOGY

Comprehensive reviews of both the recent approaches used to quantify particle morphology and the interpretative difficulties that often ensue from the use of such

0037–0746/83/1000–0655 $02.00

methods, are presented elsewhere (Barrett, 1980; Beddow, 1980; Meloy, 1980; Clark, 1981; Kaye, 1981a; Orford, 1981). In general, to judge by the plethora of available shape/form indices in the geological literature (Orford, 1981), it appears that the problem of reducing the two-dimensional variations of the particle's outline on to a linear scale has proved intractable to a complete solution. The relative importance of particle form in explaining detrital sedimentation invariably depends on the success of the investigator in using one of a number of morphometric-based techniques which are said to characterize particle form successfully. Most of these techniques rely on the identification of major linear axes of particle size in either two or three dimensions (thin-section or free grain) which, when represented by means of dimensionless ratios, are assumed to specify the form (usually as shape or sphericity) of the particle's morphological envelope in terms of similarity to standard reference outlines or solids such as the sphere or ellipsoid. However, most investigators can cite situations where particles defied morphological description in terms of such axial ratios and form indices, such that adequate specification of detrital particle morphology is not the general rule in sedimentological studies. These morphological characterization inadequacies are most prominent when dealing with recently weathered particles, as well as indurate, diagenetically altered particles observed under thin section analysis. (See, for example, May's (1980) comments concerning the difficulties that Crook (1968) encountered when producing a non-quantitative typology of possible quartz grain forms resulting from weathering by alkaline groundwater chemical etching.)

A problem often encountered during the description of irregular particles is the presence of a jagged-edge morphology and/or a crenellate-edge morphology on the particle outline. The presence of either morphology leads to a notched outline with the notches referred to as re-entrants. Re-entrants can result in radical deviations between the actual particle outline and the convex regularity assumed by the reference solid associated with the particular morphological index under consideration. Figure 1(A) shows an example of a quartz grain with major re-entrants, and clearly any description of this example in terms of axis lengths or axial ratios would be insufficient for particle morphological specification. Even a switch to direct indices of angularity/roundness (Wadell, 1933; Cailleux, 1947; Lees, 1964) fails to specify morphology adequately in the presence of re-entrants, due to the

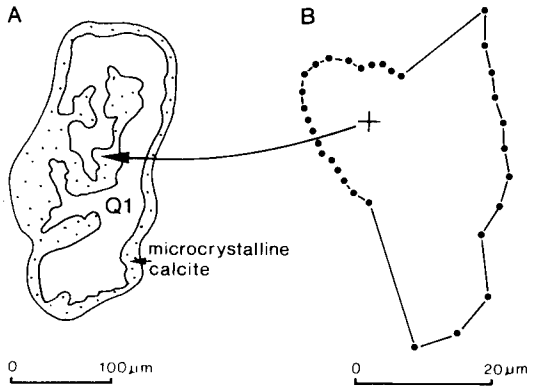

Fig. 1. The difficulty that re-entrant morphology causes in particle form characterization. (A) A carbonate-cemented pure quartz sandstone particle with crenellate morphology. (B) The reconstructed particle outline based on the first boundary intersection on radial lines from the particle's centre of gravity. Taken from a thin section after Alimen (1944).

complexity and difficulty of obtaining unequivocal and representative component measurements required in the computation of such indices. Reviewers of roundness indices tend to stress the essential subjectivity and time-consuming nature of calculating even semi-efficient indices related to angularity/roundness (Lees, 1964; Barrett, 1980; Orford, 1981).

By far the most successful technique of the last decade used for analysing irregular as well as regular grain morphologies, both in terms of grain shape and roughness, is that body of analytical techniques which decompose the unrolled outline of a grain's silhouette into a series of fundamental harmonic and subharmonic wavelengths. The principle analytical method used for this end is that of Fourier analysis (Ehrlich & Weinberg, 1970; Ehrlich *et al.*, 1980; Clark, 1981), although other mathematical functions such as Walsh, Haar and Rademacher have been suggested as a means of countering some of the problems identified with the use of Fourier decomposition (Beddow, 1980; Meloy, 1980).

Despite the successes achieved by Ehrlich and his colleagues in discriminating between sedimentary environments on the basis of particle morphological profiles, it is important to note that decomposition techniques work best with particles that are basically regular in a macro-sense. Grain textures and particle roughness can be extreme but, as scale edge effects, they are monitored by high-order harmonics and do not disturb the basic particle shape analysis provided by the lower harmonics. When the macro-shape of the

particle begins to show irregularities that are manifest in a re-entrant morphology then the harmonic specification at lower harmonics is not always unambiguous. Figure 1(A) gives an example of this type of aberrant particle morphology taken from a thin section of a carbonate-cemented quartz sandstone (Alimen, 1944). The quartz grain has been chemically etched and dissolved silica replaced by microcrystalline calcite. Form analysis by the conventional method of fitting a Fourier series to the outline requires the length of radial lines from the particle's centre to the particle's boundaries, as the input data for particle description. Under this assumption, radials can only intersect the particle boundary once, hence the problem presented by multiple boundary intersections occurring with re-entrant morphologies. Figure 1(B) is the reconstructed profile of Fig. 1(A), on the basis of first radial intersections only. Clearly there are substantial differences between the two images (Fig. 1A, B), even to the point that the reconstructed grain of Fig. 1(B) is not even a part of the quartz grain, but is centred on a re-entrant space! Alternative methods of calculating the initial data series from the original grain outline have been advocated which avoid the radial boundary problem (Zahn & Roskies, 1972), but there is little sign of their use in the geological literature.

Studies of detrital grains can only be enhanced if the morphology of those grains traditionally regarded as irregular can be quantitatively assessed with accuracy. The rest of this paper is therefore concerned with presenting the concept of *Fractal Dimension* and its use in characterizing particle morphology. The ability of this technique to specify morphology improves as the particle outline becomes more irregular. This appears to be the first index that specifically caters for the form description of highly irregular grains.

FRACTAL DIMENSION

A method by which particle form could be established is based on the change in orientation of chords of the particle's perimeter when it is expressed as a two-dimensional surface outline (Clark, 1981). The practice of assessing form based on a 2-D projected surface is not unusual and in many cases (as in thin-section analysis), this perspective is the best that can be obtained. Further details of fractal analysis in this paper will consider only the 2-D perspective, though fractal characterization does not assume nor require the use of the maximum projected particle plane.

Clark (1981) indicated a number of approaches to particle form measurement, in which the variation of orientation or distribution of chords, radii or angles related to surface perimeter variation can be analysed. Piper (1971) noted that plots of distribution of angles between varying chord lengths measured around the particle perimeter could be used in estimating particle roundness. This approach, if chord length is taken to the limit, would allow a continuous functional derivative to be used to describe the surface outline. Unfortunately a major problem ensues; the calculation of derivatives for irregular (angular particles) becomes computationally difficult with increasing particle roughness, until a point is reached where the particle outline will be so irregular that no continuous function can be derived.

That class of lines and surfaces which resist the fitting of continuous functions has long been regarded by mathematicians as quirks which go against the general tide of mathematical expectation. However, during the late nineteenth century a number of mathematicians (e.g. Cantor, Peano, Hausdorff) questioned the aberrant status of non-regular surfaces and argued that nature provides more instances of irregularity than previously supposed. It is at this point that the concept of fractal dimension can be introduced effectively. The fullest review of fractal origin and development is provided by Mandelbrot (1977) who advocates that it is the only method by which non-Euclidean surfaces and lines can be accurately characterized. Kaye (1978, 1981a) provides a useful review of the use of fractals in relation to particle characterization in powder technology.

Any interpretation of what the fractal dimension of a line represents is best seen in a semi-empirical fashion, as was first recognized by Mandelbrot (1977) based on his interpretation of Richardson's work on the paradox presented by measuring coastline lengths. Richardson's unpublished study from the beginning of the twentieth century, concerned the measurement of coastlines and the effect, later known as the Steinhaus paradox (Steinhaus, 1954), by which the smaller the unit of measurement, the longer the perimeter length of the same fixed coastline length appears to become.

Figure 2 exhibits this principle and is based on Mandelbrot's redrawing of Richardson's data. It appears that if the length of a fixed irregular perimeter (P) is measured repeatedly in terms of the number of fixed measurement units or step lengths (S) required

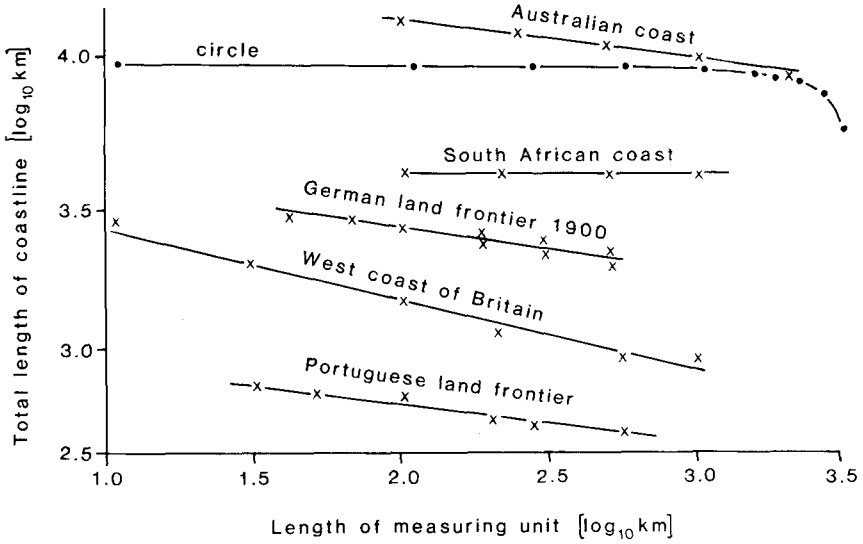

Fig. 2. The relationship between length of measuring unit and the apparent length of coastline when measured by the unit length. Mandelbrot's (1977) redrawing of Richardson's unpublished data. Note the zero rate of perimeter change for Euclidean polygons, compared to decreases in perimeter for actual non-Euclidean coastlines.

to cover the outline, then the smaller the step length the longer the apparent perimeter distance. If the logarithms of both P and S are plotted jointly, then the relationship between log P and log S is markedly linear. Richardson first noted that differing national coastlines had different gradients of proportional change between P and S, but did not consider the slope term (b) to be of any theoretical interpretation. Figure 2 also shows that a Euclidean polygon (in this case a circle) does not show the same linear change but rapidly converges to some limiting value of P as S decreases. This is important as the slope of the stable element of the circle plot tends towards zero. Mandelbrot (1977), however, considers the value of b to be of significance in that it is proportional to the value of the fractal dimension (D) of the closed loop.

If the fractal value D equals the slope term plus one ($D=b+1$) then

$$\log P \propto (D-1) \log S \tag{1}$$

so that

$$P \propto S^{(D-1)} \tag{2}$$

such that D can be seen as a dimensional power of the loop. (The proportionality sign is due to the need for an intercept term before equality in eq 1 or 2 can be satisfied.) The morphological characterization of any outline can be related to the exponent of the step-perimeter relationship, according to the fractal concept.

The theoretical range of D lies between 1·0 and 2·0, hence the need for D to be scaled up by the addition of 1·0. This value of D reflects the plane filling tendencies of the 2-D outline under consideration. Consider a circle which would have $D=1{\cdot}0$ (as $b=0$); once the outline loop is closed there is no real potential for further filling of the plane's surface, upon which the loop is lying, by the loop itself (Fig. 3A). This is also true for basic variants of Euclidean polygons (e.g. Fig. 3B) where $D \rightarrow 1{\cdot}0$). The dimension of a plane is 2·0, therefore the nearer a closed loop fills all the space of its outscribed plane, the closer to 2·0 the equivalent fractal value reaches. Figures 3(C, D) shows stages of increasing convoluted irregularity by which plane space filling takes place. Mandelbrot argues that Brownian motion (random variation) is the best example of a line which will have a D value approaching 2·0. The more irregular the particle outline, the closer to 2·0 will be the value of D.

The response between particle outline variation and fractal dimension has not yet been specified, though Flook (1978, 1979), Kaye (1978, 1980, 1981a, b), Schwarz & Exner (1980), Whalley & Orford (1983) and Orford & Whalley (1983) have given examples of its use with particle morphology. Figure 4 shows schematically the possible response curves of D related

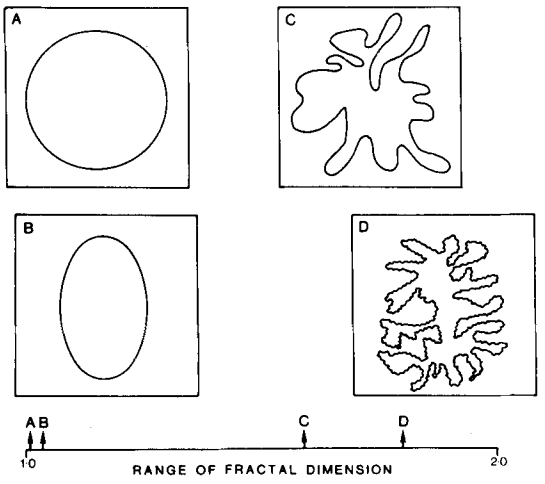

Fig. 3. The range of the fractal dimension between 1·0 and 2·0 delineates the differences between regular Euclidean figures ($D = 1{\cdot}0$) and non-Euclidean, non-regular and random plane filling figures ($D \rightarrow 2{\cdot}0$).

to loop characterization ranging from Euclidean to random curves. Initial empirical evidence (Whalley & Orford, 1983) indicates that the most likely response curve is that which shows little variation in D for relatively major changes in basic Euclidean particle shape. Yet there is the compensation that this same response curve shows a greater sensitivity by fractal analysis in morphological characterization of roughness and textural variation associated with highly irregular curves (i.e. particle outlines).

DERIVATION OF FRACTAL DIMENSION

Fractal values can be obtained by hand measurement using dividers and varying the step lengths to encompass the projected particle perimeter. Schwarz & Exner (1980) used a semi-automatic method of calculating fractals requiring a Kontron Videoplan image analyser. Results in this paper were obtained by both Videoplan and by the automatic method outlined by Telford *et al.* (1983). The nature of the fractal technique is such that the scale of the particle outline used should not effect the D value, except allowing more precision to be obtained as image enhancement allows small S definition. The linearity of the log P–log S relationship is evidence for the presence of 'self-similarity' in scales of particle morphology at all measurement sizes (Mandelbrot,

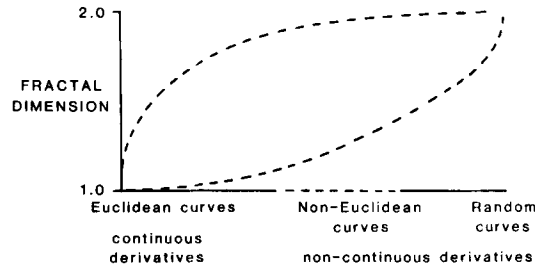

Fig. 4. Envelope of response between fractal value and variation in particle form. Evidence suggests that the true response line lies towards the lower limb of the envelope, i.e. fractals represent a better discriminating index for non-Euclidean curves.

1982), but as we shall note later, this concept can break down such that curvilinear log P—log S relationships occur with some particles. The hand method of step-length measurement can be speeded up by using an x–y digitizer on the particle outline, thus allowing rapid computation of S and P. The problem of hand wobble associated with hand digitization means that D values in the zone of smallest step size may vary. Some of this effect can be discounted by the use of least-squares linear regression to fit the fractal line to the data. This problem is further diminished, or objectively standardized, by using a video-based image analyser to obtain the boundary co-ordinates of the particle's outline (Telford *et al.*, 1983). This latter method enables an image of the particle outline to be automatically transferred into a digital matrix, recording either the particle's presence/absence in every one of a maximum 200×200 pixel (picture element) grid. Figure 5 shows a schematic

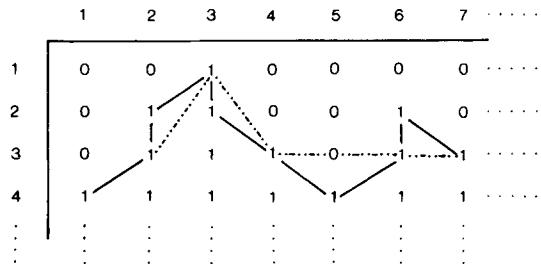

Fig. 5. Digisector matrix of presence (1) or absence (0) of particle form, taken from a video image of a particle which has been analysed by an Apple II microprocessor for grey level variation. Two levels are selected and the contour boundary between the two levels is defined as the boundary of the particle's outline. Solid lines indicate the step separation of 1 pixel, and dotted line indicates step separation of 2 pixels. The ith step length is expanded by 1 pixel per step.

view of this digitized grid held by an Apple II microcomputer, where 0 or 1 reflects the absence or presence of the particle image. It is a simple sequential computational operation to calculate P based on the number of steps round the profile, where step length starts with the distance between adjacent pixels and then is expanded by one pixel distance per new step length, i.e. $S_i = i$ pixels length.

Two problems arise from this approach; step lengths are not always equal due to the problem of varying adjacent pixel orientation around the particle perimeter having variable distances. Schwarz & Exner (1980) suggest that in the long run, given sufficient steps, the difference in actual step length for any *S per se*, will be averaged out. (The final value of S is given by $\bar{S}$ for any P_i value.) To avoid major step differences they recommend that only step lengths between 0·085 and 0·25 of the particle's A-axis length be used in the computation of D. The second problem relates to the probability of closing the loop of step measurements with a final reduced step length. The loss of accuracy of any estimate of P is, however, marginal for the smallest step lengths. The closing gap error encountered with the largest step lengths may explain the rapid decrease in estimated P at these larger S-levels. This problem has been considered by us as a possible cause of non-linearity in the log P–log S plot (see below).

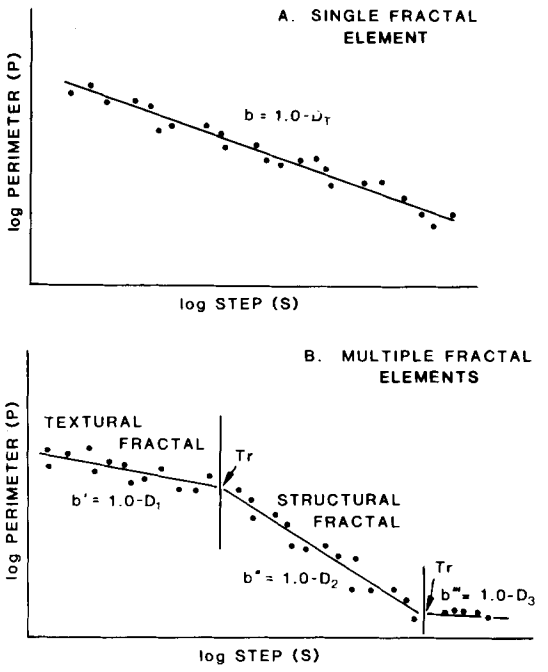

Fig. 6. Fractal elements. (A) Single element overall represented by D_T. (B) Multiple elements represented by D_1 (textural fractal), and D_2 (structural fractal). T_r marks the boundary between the textural and the structural fractal domains.

FRACTAL ELEMENTS

Mandelbrot (1977) and Kaye (1978) assert that the fractal value relates to the slope of the best fit line within the log P–log S plot (see Fig. 6A), thus identifying a single fractal with an overall *single* dimension (defined by us as D_T). There are areas of the plot which were regarded by both as showing non 'self-similarity' (i.e. non-linear elements of the plot) and therefore of no theoretical use. Mandelbrot (1977, 1982) advocates that, in theory, fractals reflect self-similarity of the morphological variation of the curve under analysis. In short, self-similarity can be regarded as implying that at all scales of examination the outline shows the same relative variation of morphology. As a working view of sedimentary particle morphology this proposition has not been found to be true (Kaye, 1980). Although examples of slight non-linearity have been thought to relate to the particular fractal generating algorithm used (M. Clark, 1982, personal communication), and there is evidence that curvilinearity of the plot at the largest step values obtained can be induced by Schwarz & Exner's (1980) algorithm, there does appear to be wider empirical evidence (Flook, 1979; Orford & Whalley, 1983) that at times two linear elements appear on the fractal plot. These two linear units represent two separate fractal elements (Fig. 6B); D_1 related to the smallest step lengths and referred to by Kaye (1978) and Flook (1979) as the *textural* fractal, as this element monitors the smallest edge effects on the out-line. Flook labelled the second element (D_2) as the *structural* fractal, as it refers to the macro-scale element of the particle, i.e. particle shape. The use of two fractal values implies that the particle shows two separate 'self-similar' scales of surface morphology inherent in the particle outline. To date, no investigations have undertaken tests of statistical difference between the fractal regressions or fractal values to see whether there is a substantive difference between the slopes of the two fractal models.

Fractal elements have been established by us by fitting linear elements to visually defined ranges of S-lengths (domains) associated with obvious linear units of the overall fractal curve. This visual fractal fitting can lead to problems. It can be argued that the

intersection of any two linear elements should coincide with the domain boundary, i.e. that the hinge point of the two elements occurs on the domain value. Empirically this has not always been the case and may reflect either an invalid choice of domain range, or the need for further intervening linear elements between the two under analysis. This latter point reflects the way in which scales of particle morphology with measurable size are observed, when a range of self-similar elements would be needed to model the fractal change. Alternatively, given sharp breaks of scale-dependent variation, then the fitting of double fractal boundary positions becomes easier. At this stage we have made use of Schwarz & Exner's (1980) algorithm which makes no assumptions about the manner or number of fractal elements to be extracted. This led us to make a conscious decision to employ the two-element model only. A third element has been observed on occasions associated with the largest *S*-lengths, but it has not been used as it may be an artefact of the algorithm's closure problem (Fig. 6B).

We have defined the boundary of the two fractal model as T_r (where $T_r = S/H_{max}$, S is the step length at the boundary and H_{max} is the particle's A-axis length). It should be noted that occasionally the value reported of D_T is smaller/bigger than either D_1 or D_2. This reflects the calculation of D_T from within the window of $0{\cdot}085$–$0{\cdot}5H_{max}$, whereas the visual calculation of D_1 and D_2 can depend on the step lengths outside of this window.

Although it may go against the spirit of fractal self-similarity as proposed by Mandelbrot (1982), some particles may well show continuous gradients of fractal change. Under these circumstances morphological variation is dependent on measurement scale. Rather than use multiple fractal elements, which will only approximate the rate of change, it may be better to use a continuous function such as the second derivative of log P as a function of log S. Curvilinear regression may be a way of deriving this type of function, though a weighted least squares approach may be needed (M. Clark, 1982, personal communication) due to the variable spread of data found in the log P–log S plot (see Fig. 7).

The relative steepness of fractal element slopes indicates the possibility of three types of fractal assemblage. This typology assumes that only textural and structural fractals occur. Figure 8 identifies the three basic types: type I is the standard single fractal population which is commonly associated with relatively regular outlines, in the sense that macroshape dominates the particle and no, or very little, real edge roughness is observed. Type II shows a convex fractal structure with a more irregular dominant structural nature and minor, or no real observable edge texture. The quartz particle in Fig. 1 is an example from this type with $D_T = 1{\cdot}19$, $D_1 = 1{\cdot}05$ and $D_2 = 1{\cdot}34$. Type III particles exhibit very marked irregular edge texture relative to a more regular structural outline, while the sub-fractal plot shows a concave nature.

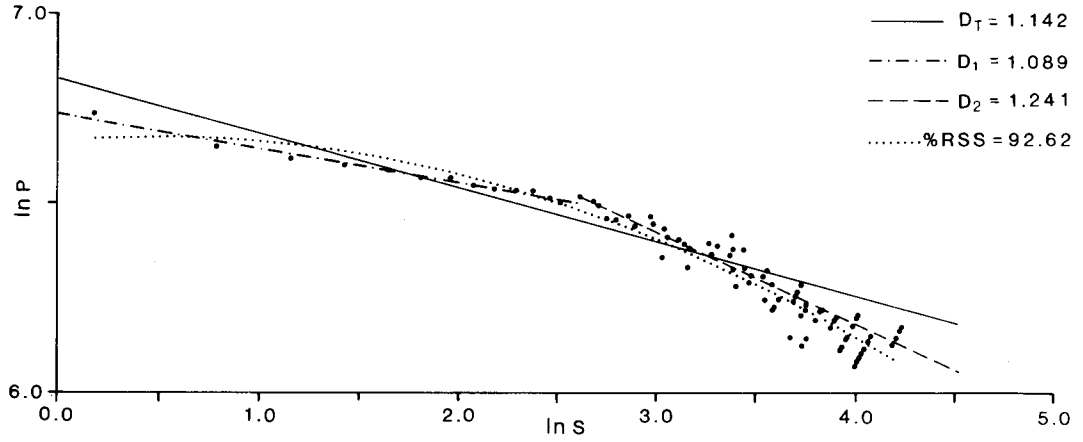

Fig. 7. Example of fractal plot of a quartz grain (not shown) showing the problem of locating fractal element domains. D_T is found by a least squares linear regression for all data points. D_1 and D_2 are least squares fit to ranges selected by eye. %RSS refers to the fit of a quadratic polynomial equation to aid fixing domain boundaries (see text). Note the skewed fitting of this unweighted regression estimate.

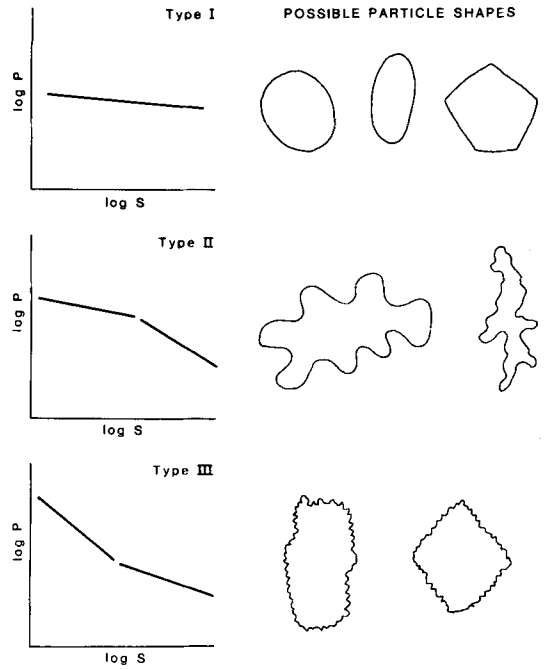

Fig. 8. Combination of fractal elements which allow identification of three types of fractal structure. Examples of particle types associated with the assemblage types are suggested.

CALIBRATION OF FRACTAL DIMENSION

The value of using fractals to index particle morphology will depend on calibrating the relationship between changing morphology and changing fractal value. Figure 9 is an example of how fractal population structure and value varies with changing particle morphology Particle sets 1a to 1f, and 2a to 2f, show two basic particle forms (circle and ellipse) with a superimposed progressive macro-scale crenellate-edge morphology, but without micro-scale edge texture effects.

It is clear that all fractal population values generally increase with increasing particle irregularity, though the greatest rate of change in overall and structural fractal is commensurate with the more prominent jaggedness introduced by crenellate morphology. On this set of particles no real discrimination of textural fractal is observed, while the structural fractal is clearly discriminatory (within the range 1·0–1·5). These results are not surprising given the lack of micro-texture on the profile. Values of D_T rise commensurate with the increase in D_2. There appears to be little difference between shape types a, b and c in terms of fractal values, while there is also no real discrimination between the basic circle/ellipse. This is to be expected given their regular Euclidean geometry. The value of D_T is shown to be limited when it is clear that D_1 and D_2 are evident. But these results also argue for the need to state D_1 and D_2 values, even when D_T appears to be the only viable fractal (i.e. type I population).

Although textural fractal appearance is limited on the calibration particles, this is not necessarily solely related to the smoothness of the particle profiles at a micro-level. Examples of particles with highly roughened edge textures at the micro-scale are shown in Fig. 10. The carbonate beach grains from Male Atoll in the Maldives are detrital particles of coral and algae. Many of the indentations reflect the cellular structure of the fragments, and would, *a priori*, be expected to generate a high textural fractal value. Yet all of the grains are within the range of the smoother calibration particles. Similar low textural fractal values are recorded for the glassy pyroclastic particles obtained from the 1980 Mount St Helen's eruption (Fig. 10). The outlines are apparently roughened but reflect multiple facets of an irregular particle projected on to one surface and therefore may at first glance be seen to reflect the glassy composition of the ejecta. However, the fractal is based on the outline *per se* and yet does not appear to monitor the apparent roughness exhibited. These results suggest to us that the indentations of particle form which register against the textural fractal must be on a scale larger than the micro-indentations shown by these particles, but at the same time must be on a scale which is not related to particle structure. The T_r value between the fractal elements indicates the potential scale of textural elements as anywhere between 0·04 and 0·14 of the particle's *A*-axis.

DISCRIMINATION OF PARTICLE POPULATIONS BY FRACTAL ANALYSIS

Principles

An important requisite of any form index is its capacity for discrimination of both obvious and subtle particle morphological differences. The value of fractal analysis will therefore depend on its discriminatory power in a geological context that would be

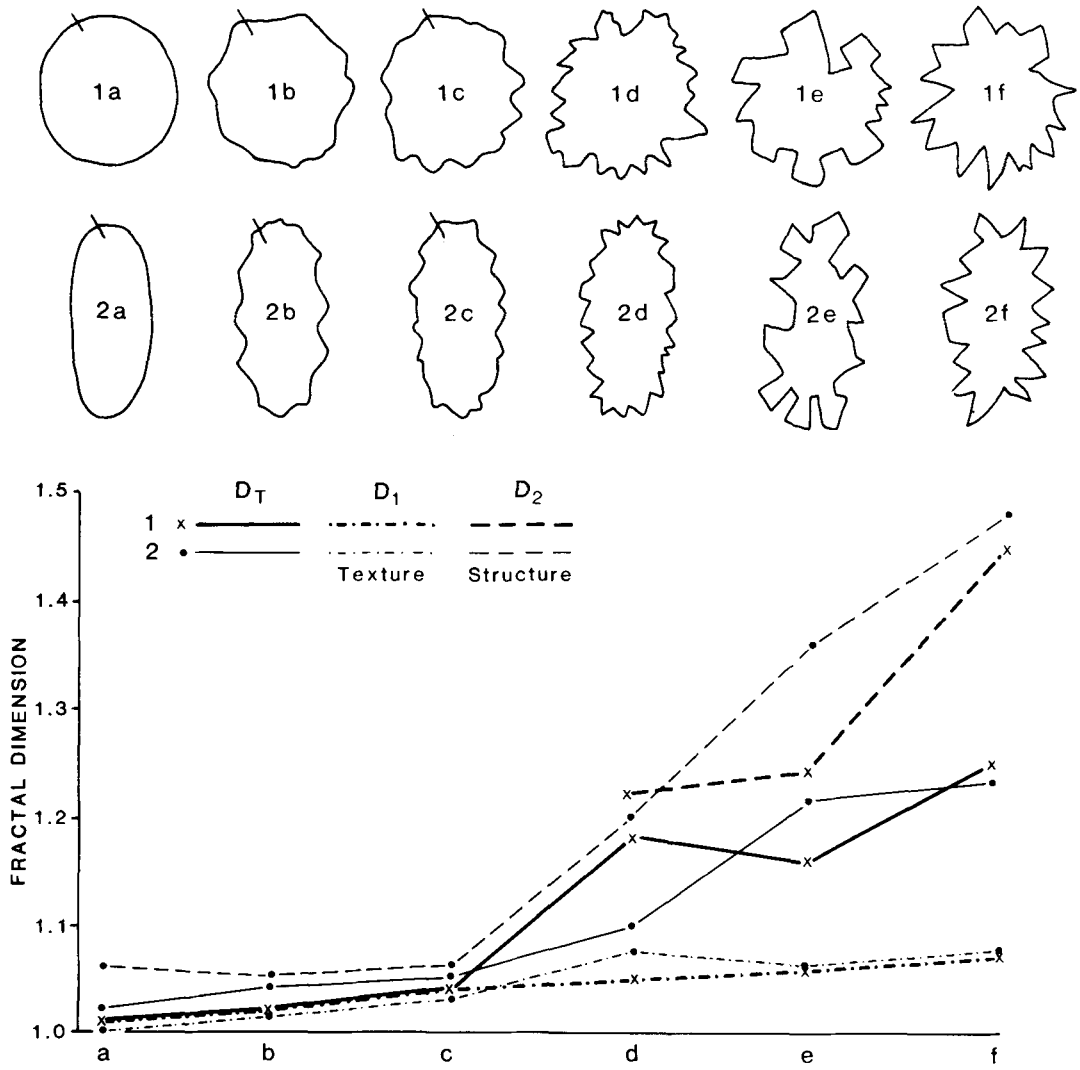

Fig. 9. Calibration of fractal values against increasing crenellation (jaggedness) of particle outlines. Note that the best morphological characterization power resides in the D_T and D_2 values, the latter value related to the structural element of the particle form. The lack of D_1 power is due to the absence of textural effects from the particle outlines. Note that best characterization in terms of discrimination by fractal analysis is when particles exhibit irregularity of outline.

contentious for other methods/indices of morphological analysis. Figure 11 illustrates this type of problem. The particle outlines have been taken from a thin section of a tectonically deformed radiolarian chart (Cayeux, 1929). The deformed radiolaria are composed of a micro-granular quartz, set in a matrix of granular ferruginous quartz. It is readily apparent that the radiolarian casts have been variably deformed and chemically etched, such that some grains (e.g. R9) show relatively little differentiation with radiolarian spikes still prominent while, at the other extreme, highly irregular fragments show evidence of major mineral disturbance and replacement (e.g. R10).

Cayeux's original section shows two aspects which are not included in Fig. 11, and which would effect any population estimates of particle morphology. First, far more fragments of radiolaria are exhibited on Cayeux's section than used in this example. Their

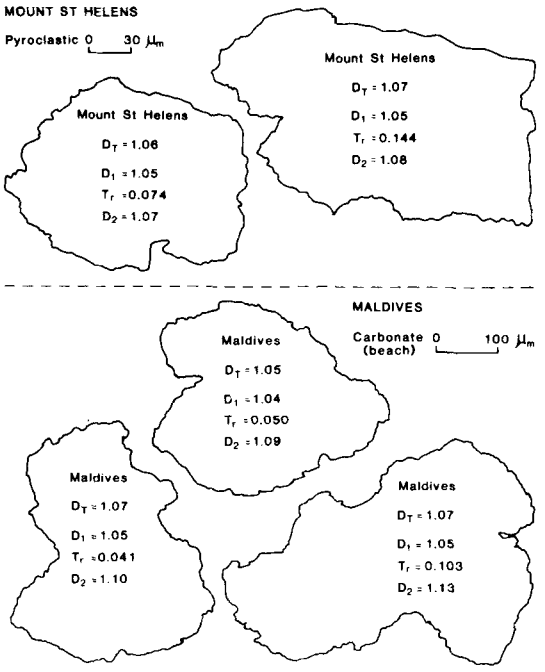

Fig. 10. Examples of fractal analysis for carbonate beach grains from the Maldives and pyroclastic particles from Mount St Helens Eruption (1980).

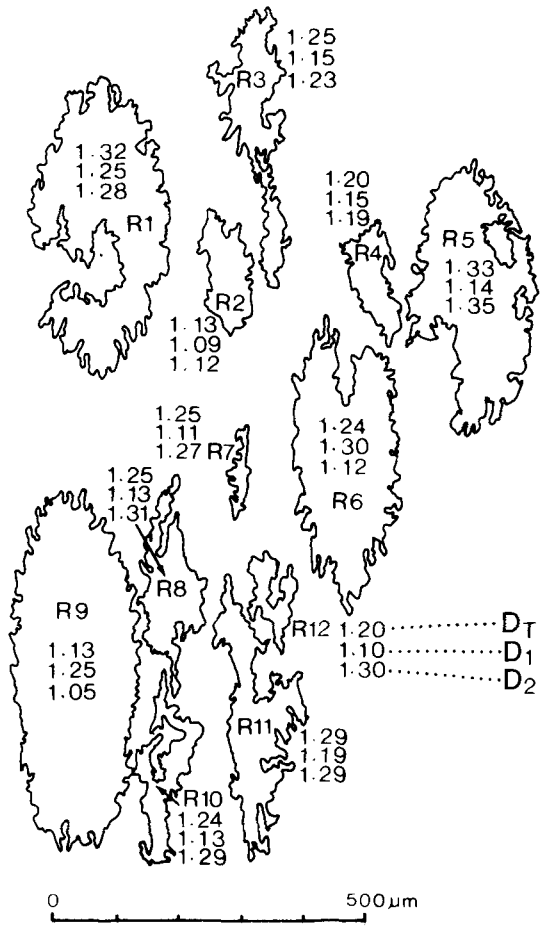

Fig. 11. Highly irregular particle outlines used for fractal analysis and discrimination of particle types by fractal structure. The images are taken from a thin section of a tectonically deformed radiolarian chart composed of microgranular quartz set in a matrix of granular ferruginous quartz. D_T, D_1 and D_2 refer to fractal element values.

absence is not related to any problem of fractal failure *per se*, but more to the problem of lack of section magnification for accurate fractal measurement. Secondly, and of greater importance, is that many of the particles in the original section have islands of ferruginous quartz within the radiolaria casts. These reflect sectioning of 3-D mineral replacement structures by the particular thin section plane. Fractal analysis as proposed by Schwarz & Exner's algorithm, and used in this paper, requires a single closed profile loop, so that internal 'island' cannot be analysed. This is a major limitation for this version of fractal analysis, though not insurmountable as Mandelbrot (1982) approaches the problem of fractal analysis by fitting combinations of polygons, with a basic shape and a constant proportional reduction in size, to the required outline (Koch island fitting) and thereby accommodates potential gaps in the profile envelope. The rate of polygonal reduction required to fill the profile can be used to theoretically evaluate D_T.

These two problems aside, the re-entrant and crenellate morphology of the radiolarian casts would prove hazardous for conventional methods of form characterization, with even harmonic analysis foundering given the convolutions of particles like R10. The rest of this section describes the possibility of quantitatively discriminating between these particles on the basis of morphology using fractal description.

Results

Figure 11 indicates the values of D_T, D_1 and D_2 for each particle, while Table 1 presents the summary statistics for the mean, variance, range and standard error ($p = 0{\cdot}05$) associated with the sample set ($n = 12$). Although the difference between D_1 and D_2 mean

Table 1. Summary statistics of D_T, D_1 and D_2 for all particles shown in Fig. 11

	D_T	D_1	D_2
Mean	1·23	1·16	1·23
Range	1·13–1·33	1·09–1·30	1·05–1·31
Variance ($\times 10^{-3}$)	3·969	4·448	8·667
Standard error range ($p=0·95$)	1·194–1·265	1·121–1·198	1·176–1·283

values is not significant ($t_{obs}=2·027 : t_{cal}$ ($p=0·05$, $v=11)=2·074$), the marginal overlapping of standard error ranges suggests that to use D_T values by themselves may be in error and mask discrimination potential. The disparities of radiolarian morphology suggests that it may be an error to consider the sample as a homogeneous group.

Population discrimination was furthered through the use of Q-mode cluster analysis to identify possible particle morpho-facies. The three fractal values for each particle were used as object attributes in the Q-mode analysis. A dendrogram resulting from Ward's 'sum of squares' linkage method being applied to a similarity matrix of Euclidean distance between all pairs of particles, is shown in Fig. 12.

The low levels of relative group similarity (all groups identified by a relative similarity of 0·25), suggests that sub-group discrimination may be efficient (Demirmen, 1972; Orford, 1975). A visual inspection of the new sub-groups support the discriminatory efficiency of fractual technique in characterizing morphology of this particle set, given the evident within group similarities and between group differences.

Table 2 shows the mean and standard deviation of fractal populations for the four morpho-facies resolved. Group 1 comprises R1, R11 and R5, group 2 comprises R3 and R4, group 3 comprises R7, R8, R10 and R12, and group 4 comprises R2, R6 and R9.

Table 3 indicates the results of a one-way analysis of variance used to test the hypothesis of no significant difference between four morpho-facies's mean values of D_T, D_1 and D_2 respectively. As might be expected, the variation in structural fractal value engenders a highly significant difference between groups ($p \leq 0·01$). Similarly, the D_T values are also significantly

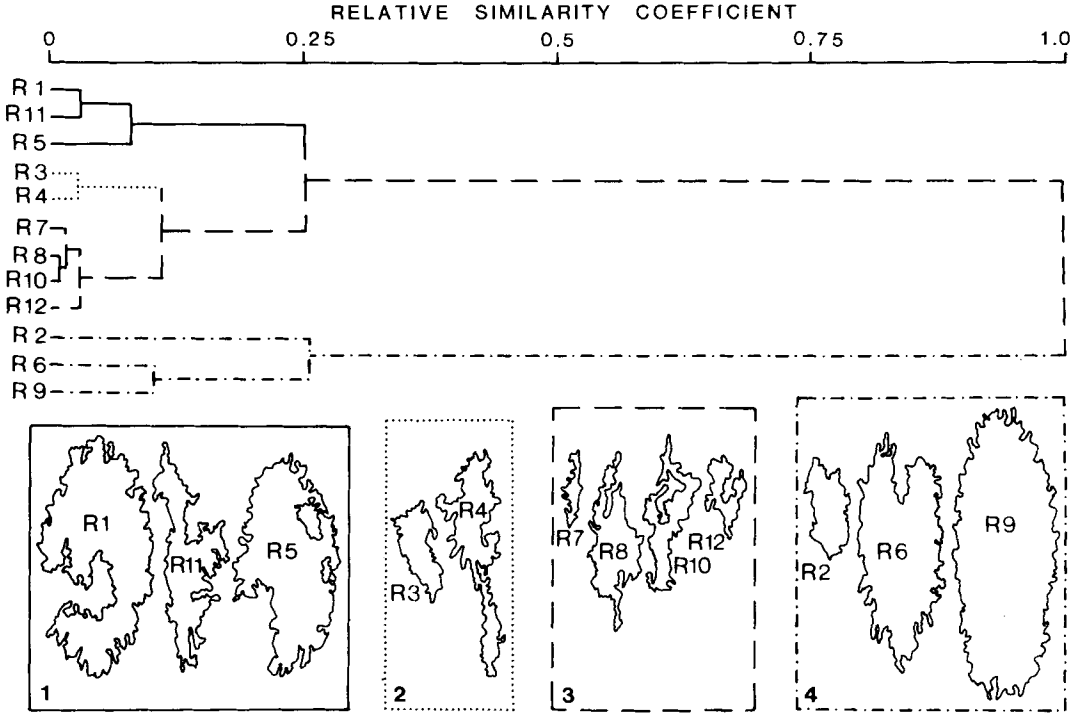

Fig. 12. Dendogram based on Ward's 'sum of squares' linkage method, to show the morpho-facies evolved from Q-mode cluster analysis of fractual values for each radiolarian particle shown in Fig. 11. morpho-facies groups 1–4 are shown left to right at the base of the diagram. Note the evident clustering of similar particle forms as a function of size and crenellation.

Table 2. Mean and variance of D_T, D_1 and D_2 for the four morpho-facies shown in Fig. 12

Morpho-facies group	D_T		D_1		D_2	
	$\bar{X}$	S^2	$\bar{X}$	S^2	$\bar{X}$	S^2
1	1·31	$4{\cdot}326 \times 10^{-4}$	1·19	$3{\cdot}025 \times 10^{-3}$	1·30	$1{\cdot}428 \times 10^{-3}$
2	1·125	$1{\cdot}246 \times 10^{-3}$	1·15	0	1·21	$7{\cdot}952 \times 10^{-4}$
3	1·235	$5{\cdot}664 \times 10^{-4}$	1·11	$2{\cdot}250 \times 10^{-4}$	1·29	$2{\cdot}924 \times 10^{-4}$
4	1·166	$4{\cdot}032 \times 10^{-3}$	1·21	$1{\cdot}205 \times 10^{-2}$	1·10	$1{\cdot}632 \times 10^{-3}$

different ($p \leq 0{\cdot}05$). The lack of statistical significance between D_1 values follows on from points made concerning calibration results. These results reinforce the proposition that fractal characterization may be feasible for heterogeneous populations of irregular particles.

Table 4 shows the significance of the morpho-facies types. If there is a statistical significance between the mean textural fractal and the mean structural fractal ($p \leq 0{\cdot}05$), then types II or III fractal populations can be inferred. The difference between the two depends on which fractal (textural or structural), is the larger. If no significance is established then type II is inferred. A *t*-test of the H_0 cited in Table 4 indicates that only groups 1 and 3 are true type II populations ($D_1 \ll D_2$), though group 2, as a type I, is tending towards type II. Only group 4 shows any tendency towards a type III population, though on significance grounds it is only a Type I structure.

Table 3. Result of testing (by one-way analysis of variance), for significant differences between mean fractal values for the four morpho-facies

H_0: There is no significant difference between morpho-facies mean fractal values

$\bar{D}_{n1} = \bar{D}_{n2} = \bar{D}_{n3} = \bar{D}_{n4}$ where n = T, 1 or 2

for D_t: $F_{obs} = 7{\cdot}313$ $p \leq 0{\cdot}05$: reject H_0
for D_1: $F_{obs} = 1{\cdot}630$ not significant: accept H_0
for D_2: $F_{obs} = 29{\cdot}77$ $p \leq 0{\cdot}01$: reject H_0
$v_1 = 3$ and $v_2 = 8$ degrees of freedom

Table 4. Results of testing (by *t*-test), for significant differences between D_1 and D_2 of each of the four morpho-facies

H_0: There is no significant difference between D_1 and D_2 for the *i*th morpho-facies

*i*th-morpho-facies group	t_{obs}	v(degrees of freedom)	Probability
1	2·936	5	0·05
2	2·977	1	Not significant
3	15·359	8	0·01
4	1·728	3	Not significant

The differences between and within both types II and III populations can be examined using a graphical method to assess the position of fractal element domains in the context of relative particle morphology (Fig. 13). Although groups 2 and 4 should not appear as they do not have significant domains, they have been included as points where boundary trends can be inferred. The fractal gradient is schematically drawn on to Fig. 13 to show the nature of the population type for each morpho-facies. Relative lengths of fractal lines reflects a weighted estimate of importance of each sub-population in the overall plot.

The T/H_{max} axis reflects the ratio between the step length at the fractal truncation point (T) and the particle's A-axis (note, log values not used). This variable indicates the standardized size of the edge textural roughness units on the particle perimeter, relative to the particle size. On the basis of this variable, group 3 particles have larger roughness

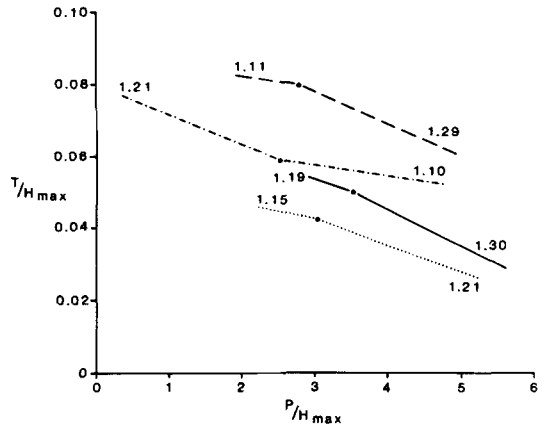

Fig. 13. A graphical means of further population type discrimination based on the relative position of fractal boundaries. T/H_{max} measures relative size of roughness elements on the particle outline, while P/H_{max} monitors the elongation of discoid qualities of the particle. Notation of morpho-facies fractal structure is the same as used in Fig. 12. Figures are values of D_1 and D_2 fractals.

elements than group 1 particles. The P/H_{max} variable is the ratio between the calculated perimeter (P) at the fractal break, and the particle's A-axis. If the fractal break is valid, this variable monitors the discoid tendencies of the basic particle form prior to edge roughness, so that a particle with a low value of P/H_{max} is likely to be more elongated than a particle with a high P/H_{max} value (i.e. group 1 compared with group 3). If group 2 is moving towards a type II population, then its elongation factor is also noted by its low T/H_{max} value. Group 4 will not be part of this set as it is tending towards a type III plot, and at this stage there is little empirical basis for advocating its structure relative to a Fig. 13 type diagram. These limited results further support the discriminatory potential of fractal values in analysing shape populations in heterogenous collections of irregular particles.

CONCLUSIONS

It appears that some of the problems of characterizing highly irregular particles for geological purposes may be overcome by the use of fractal analysis. Efficient discrimination between environments producing irregular particles based on the fractal parameters D_T and/or D_1 and D_2, in combination with measures of edge roughness like T/H_{max}, now appear probable. The numerical values of fractal parameters can be used as a means of quantitatively assessing the non-regular attrition on detrital particles, that has resisted methods to date. Given the value of harmonic analysis with respect to shape studies on relatively non-angular particles, and given the success of fractal analysis in characterizing very irregular particles, then the two techniques can be viewed as complementary, such that an adequate specification of particle form is now possible for all points on the continuum of particle form.

ACKNOWLEDGMENTS

We should like to thank NSF for financial support in allowing us to present a paper at the 'Workshop on quantitative measures in sedimentary and pyroclastic particle characterization' (Arizona 1982), upon which this paper is based. The critical reviews of this paper by Bob Ehrlich and Malcolm Clark are gratefully acknowledged, and as is usual, any mistakes are ours! The facilities offered to us by Professor L. Threadgold (Zoology Department, Queen's University, Belfast) and Dr H. Schwarz (Kontron GmbH) are also gratefully acknowledged. Thanks also to Maura Pringle, Trevor Malloy, Sharon Wright and Suzanne McWilliams for technical assistance in the preparation of this paper.

REFERENCES

ALIMEN, H. (1944) Roches gréseuses à ciment calcaire du Stampien: Etudes pétrographique. *Bull. Soc. géol. Fr., 5th Series*, **14**, 307–329.

BARRETT, P.J. (1980) The shape of rock particles, a critical review. *Sedimentology*, **27**, 291–303.

BEDDOW, J.K. (1980) Particle morphological analysis. In: *Advanced Particulate Morphology* (Ed. by J.K. Beddow and T.P. Meloy), pp. 1–84. C.R.C. Press, Florida.

CAILLEUX, A. (1947) L'indice d'émousse des grains de sable et grès. *Rev. Geomorph. dyn.* **3**, 78–87.

CAYEUX, L. (1929) Les roches sédimentaires de France—Roches siliceuse. *Mém. Carte. Géol. dét. France.* Imprimerie Nationale, Paris. 744 pp.

CLARK, M.W. (1981) Quantitative shape analysis: a review. *Math. Geol.* **13**, 303–320.

CROOK, K.A.W. (1968) Weathering and roundness of quartz grains. *Sedimentology*, **11**, 171–182.

DEMIRMEN, F. (1972) Mathematical search procedures in facies modelling in sedimentary rocks. In: *Mathematical Models of Sedimentary Processes* (Ed. by D. Merriam), pp. 81–114. Plenum Press, New York.

EHRLICH, R. & WEINBERG, B. (1970) An exact method for characterization of grain shape. *J. sedim. Petrol.* **40**, 205–212.

EHRLICH, R., BROWN, P.J., YARUS, J.M. & EPPLER, D.T. (1980) Analysis of particle morphology data. In: *Advanced Particulate Morphology* (Ed. by J.K. Beddow and T.P. Meloy), pp. 101–119. C.R.C. Press, Florida.

FLOOK, A.G. (1978) The use of dilation logic on the Quantimet to achieve fractal dimension characterisation of textural and structural profiles. *Powder Technol.* **21**, 295–298.

FLOOK, A.G. (1979) The characterization of textural and structural profiles by the automated measurement of their fractal dimensions. *2nd European Symp. Particle Characterization*, pp. 591–599.

KAYE, B.H. (1978) Specification of the ruggedness and/or texture of a fine particle profile by its fractal dimension. *Powder Technol.* **21**, 207–213.

KAYE, B.H. (1980) Fractal and shape description of the shape and surface structure of metal powders. *Int. Powder. Metall. Conf.*, Washington D.C. (mimeo).

KAYE, B.H. (1981a) *Direct Characterization of Fine Particles.* Wiley, New York. 390 pp.

KAYE, B.H. (1981b) Trends in fine particle characterization. *Plenary Lect., 4th Particle Size. Anal. Conf.*, Loughborough, England (mimeo).

LEES, G. (1964) A new method of determination of the angularity of particles. *Sedimentology*, **3**, 2–21.

MANDELBROT, B.B. (1977) *Fractals: form, chance and dimension.* W.H. Freeman, San Francisco. 361 pp.

MANDELBROT, B.B. (1982) *The Fractal Geometry of Nature*. W.H. Freeman, San Francisco. 460 pp.

MAY, R.W. (1980) Irregularly shaped quartz grains. *Sedimentology*, **27**, 325–331.

MELOY, T.P. (1980) Particle shape characterization: recent developments (review). In: *Testing and Characterizing of Powders and Fine Particles* (Ed. by J.K. Beddow and T.P. Meloy), pp. 1–48. Heyden, London.

ORFORD, J.D. (1975) Discrimination of particle zonation on a pebble beach. *Sedimentology*, **22**, 441–463.

ORFORD, J.D. (1981) Particle form. In: *Geomorphological Techniques* (Ed. by A.S. Goudie), pp. 86–90. Allen & Unwin, London.

ORFORD, J.D. & WHALLEY, B.W. (1983) The quantitative description of highly irregular sedimentary particles: the use of the fractal dimension. In: *Characterization and Quantification of Surface Features on Clastic and Pyroclastic Particles* (Ed. by J. Marshall). Proc. N.S.F. Workshop, Arizona State University. In press.

PIPER, D.J.W. (1971) The use of the D. Mac pencil follower in routine determination of sedimentary parameters. In: *Data Processing in Biology and Geology* (Ed. by J.L. Cutbill), Systematics Association Special Volume No. 3, 97–103.

SCHWARZ, H. & EXNER, H.E. (1980) The implementation of the concept of fractal dimension on a semi-automatic image analyzer. *Powder Tech.* **27**, 207–213.

STEINHAUS, H. (1954) Length, shape and area. *Colloquium math.* 1–13.

TELFORD, R.W., LYONS, M., ORFORD, J.D., WHALLEY, W.B. & FAY, D.Q.M. (1983) A low-cost, microcomputer-based image analyzing system for characterization of particle outline morphology. In: *Characterization and Quantification of Surface Features on Clastic and Pyroclastic Particles* (Ed. by J. Marshall). Proc. N.S.F. Workshop, Arizona State University. In press.

WADELL, H. (1933) Sphericity and roundness of rock particles. *J. Geol.* **41**, 310–331.

WHALLEY, W.B. (1972) The description and measurement of sedimentary particles and the concept of form. *J. sedim. Petrol.* **42**, 961–965.

WHALLEY, W.B. & ORFORD, J.D. (1983) Analysis of S.E.M. images of sedimentary particle form by fractal dimension and Fourier analysis methods. *Scanning Electron Microsc. 1982*, **II**, 639–647.

WINKELMOLEN, A.M. (1982) Critical remarks on grain parameters, with special emphasis on shape. *Sedimentology*, **29**, 255–266.

ZAHN, C.T. & ROSKIES, R.Z. (1972) Fourier descriptors for plane closed curves. *I.E.E.E. Trans. Comp.* **C 21**, 269–281.

(*Manuscript received August 1982; revision received February 1983*)